The mistery of mass

Ionut-Cristian Arsene

June 8, 2006

Contents

1 The Standard Model before electroweak symmetry breaking

The Glashow-Weinberg-Salam electroweak theory which describes the electromagnetic and weak interactions between quarks and leptons, is a Yang-Mills theory based on the symmetry group $\mathrm{SU(2)_L} \times \mathrm{U(1)_Y}$. Combined with the $\mathrm{SU(3)_C}$ based QCD gauge theory which describes the strong interactions between quarks, it provides a unified framework to describe these three forces of Nature: the Standard Model. The model, before introducing the electroweak symmetry breaking mechanism, has two kinds of fields.

There are first the matter fields, that is, the three generations of left-handed and right-handed chiral quarks and leptons, $f_{L,R} = \frac{1}{2}(1 \mp \gamma_5) f$. The left-handed fermions are in weak isodoublets, while the right-handed fermions are weak isosinglets

$$
I_f^{3L,3R} = \pm\frac{1}{2}, 0: \quad
\begin{array}{llll}
L_1 = \begin{pmatrix} \nu_e \\ e^- \end{pmatrix}_L, & e_{R_1} = e_R^-, & Q_1 = \begin{pmatrix} u \\ d \end{pmatrix}_L, & u_{R_1} = u_R, \quad d_{R_1} = d_R \\
L_2 = \begin{pmatrix} \nu_\mu \\ \mu^- \end{pmatrix}_L, & e_{R_2} = \mu_R^-, & Q_2 = \begin{pmatrix} c \\ s \end{pmatrix}_L, & u_{R_2} = c_R, \quad d_{R_2} = s_R \\
L_3 = \begin{pmatrix} \nu_\tau \\ \tau^- \end{pmatrix}_L, & e_{R_3} = \tau_R^-, & Q_3 = \begin{pmatrix} t \\ b \end{pmatrix}_L, & u_{R_3} = t_R, \quad d_{R_3} = b_R
\end{array}
$$

The fermion hypercharge, defined in terms of the third component of the weak isospin I_f^3 and the electric charge Q_f in units of the proton charge $+e$, is given by $(i = 1, 2, 3)$

$$
Y_f = 2Q_f - 2I_f^3 \Rightarrow Y_{L_i} = -1, Y_{e_{R_i}} = -2, Y_{Q_i} = \frac{1}{3}, Y_{u_{R_i}} = \frac{4}{3}, Y_{d_{R_i}} = -\frac{2}{3}
$$

Moreover, the quarks are triplets under the $\mathrm{SU(3)_{(C)}}$ group, while leptons are color singlets. This leads to the relation

$$
\sum_f Y_f = \sum_f Q_f = 0
$$

which ensures the cancellation of chiral anomalies within each generation, thus, preserving the renormalizability of the electroweak theory.

Then, there are the gauge fields corresponding to the spin-one bosons that mediate the interactions. In the electroweak sector, we have the field B_μ which corresponds to the generator Y of the $\mathrm{U(1)_Y}$ group and the three fields $W_\mu^{1,2,3}$ which correspond to the generators T^a [with $a = 1, 2, 3$] of the $\mathrm{SU(2)_L}$ group; these generators are in fact equivalent to half of the non-commuting

2×2 Pauli matrices

$$T^a = \frac{1}{2}\tau^a; \tau_1 = \begin{pmatrix} 0 & 1 \\ 1 & 0 \end{pmatrix}, \tau_2 = \begin{pmatrix} 0 & -i \\ i & 0 \end{pmatrix}, \tau_3 = \begin{pmatrix} 1 & 0 \\ 0 & -1 \end{pmatrix}$$

with the commutation relations between these generators given by

$$[T^a, T^b] = i\epsilon^{abc}T^c.$$

In the strong interaction sector, there is an octet of gluon fields $G_\mu^{1,\dots,8}$ which correspond to the eight generators of the $\mathrm{SU(3)_C}$ group and which obey the relations

$$[T^a, T^b] = if^{abc}T_c$$

with

$$\mathrm{Tr}[T^a T^b] = \frac{1}{2}\delta_{ab}$$

where the tensor f^{abc} is for the structure constants of the $\mathrm{SU(3)_C}$ group. The field strengths are given by

$$\begin{aligned} G^a_{\mu\nu} &= \partial_\mu G^a_\nu - \partial_\nu G^a_\mu + g_s f^{abc} G^b_\mu G^c_\nu \\ W^a_{\mu\nu} &= \partial_\mu W^a_\nu - \partial_\nu W^a_\mu + g_2 \epsilon^{abc} W^b_\mu W^c_\nu \\ B_{\mu\nu} &= \partial_\mu B_\nu - \partial_\nu B_\mu \end{aligned}$$

where g_s, g_2 and g_1 are, respectively, the coupling constants of $\mathrm{SU(3)_C}$, $\mathrm{SU(2)_L}$ and $\mathrm{U(1)_Y}$.

The SM Lagrangian, without mass terms for fermions and gauge bosons is then given by

$$\mathcal{L}_{\mathrm{SM}} = -\frac{1}{4}G^a_{\mu\nu}G^{\mu\nu}_a - \frac{1}{4}W^a_{\mu\nu}W^{\mu\nu}_a - B_{\mu\nu}B^{\mu\nu}$$
$$+ \overline{L}_i i D_\mu \gamma^\mu L_i + \overline{e}_{R_i} i D_\mu \gamma^\mu e_{R_i} + \overline{Q}_i i D_\mu \gamma^\mu Q_i + \overline{u}_{R_i} i D_\mu \gamma^\mu u_{R_i} + \overline{d}_{R_i} i D_\mu \gamma^\mu d_{R_i}$$

where D_μ is the covariant derivative which, in the case of quarks, is defined as

$$D_\mu \psi = \left(\partial_\mu - i g_s T_a G^a_\mu - i g_2 T_a W^a_\mu - i g_1 \frac{Y_q}{2} B_\mu\right)\psi$$

2 Spontaneous symmetry breaking

From the previous section, one can see that our Lagrangian doesn't describe the physical reality since the $W^\pm$ and Z bosons must have masses. In order to generate masses, we need to break the gauge symmetry in some way; however, we also need a fully symmetric Lagrangian to preserve renormalizability. A posible solution to this dilemma, is based on the fact that it is posible to get non-symmetric results from an invariant Lagrangian.

Let us consider a Lagrangian, which:

- Is invariant under a group G of transformations.

- Has a degenerate set of states with minimal energy, which transform under G as the members of a given multiplet.

If one arbitrarily selects one of those states as the ground state of the system, one says that the symmetry becomes spontaneously broken.

A well-known physical example is provided by a ferromagnet: although the Hamiltonian is invariant under rotations, the ground state has the spins aligned into some arbitrary direction. Moreover, any higher-energy state, built from the ground state by a finite number of excitations, would share its anisotropy. In a Quantum Field Theory, the ground state is the vacuum. Thus, the SSB mechanism will appear in those cases where one has a symmetric Lagrangian, but a non-symmetric vacuum.

3 The Higgs mechanism in the Standard Model

In the following section we are going to use the Goldstone theorem. We need to generate masses for the three gauge bosons $W^{\pm}$ and Z but the photon should remain massles and QED must stay an exact symmetry. Therefore, we need at least 3 degrees of freedom for the scalar fields. The simplest choice is a complex SU(2) doublet of scalar fields ϕ

$$\Phi = \begin{pmatrix} \phi^+ \\ \phi^0 \end{pmatrix}, Y_\phi = +1$$

To the SM Lagrangian discussed previously, we need to add the invariant terms of the scalar field part

$$\mathcal{L}_S = (D^\mu \Phi)^\dagger (D_\mu \Phi) - \mu^2 \Phi^\dagger \Phi - \lambda (\Phi^\dagger \Phi)^2$$

For $\mu^2 < 0$, the neutral component of the doublet field Φ will develop a vacuum expectation value

$$\langle \Phi \rangle_0 \equiv \langle 0|\Phi|0\rangle = \begin{pmatrix} 0 \\ \frac{v}{\sqrt{2}} \end{pmatrix}, \text{with} v = \left(-\frac{\mu^2}{\lambda}\right)^{1/2}$$

Now we can write the field Φ in terms of four fields $\theta_{1,2,3}(x)$ and $H(x)$ at first order:

$$\Phi(x) = \begin{pmatrix} \theta_2 + i\theta_1 \\ \frac{1}{\sqrt{2}}(v + H) - i\theta_3 \end{pmatrix} = e^{i\theta_a(x)\tau^a(x)/v} \begin{pmatrix} 0 \\ \frac{1}{\sqrt{2}}(v + H(x)) \end{pmatrix}.$$

By making a gauge transformation on this field in order to move to the unitarity gauge

$$\Phi(x) \to e^{-i\theta_a(x)\tau^a(x)}\Phi(x) = \frac{1}{\sqrt{2}}\begin{pmatrix} 0 \\ v + H(x) \end{pmatrix}$$

and then fully expand the term $|D_\mu\Phi|^2$ of the Lagrangian $\mathcal{L}_S$

$$\begin{aligned} |D_\mu\Phi|^2 &= \left|\left(\partial_\mu - ig_2\frac{\tau_a}{2}W_\mu^a - ig_1\frac{1}{2}B_\mu\right)\Phi\right|^2 \\ &= \frac{1}{2}\left|\begin{pmatrix} \partial_\mu - \frac{i}{2}(g_2W_\mu^3 + g_1B_\mu) & -\frac{ig_2}{2}(W_\mu^1 - iW_\mu^2) \\ -\frac{ig_2}{2}(W_\mu^1 + iW_\mu^2) & \partial_\mu + \frac{i}{2}(g_2W_\mu^3 - g_1B_\mu) \end{pmatrix}\begin{pmatrix} 0 \\ v + H \end{pmatrix}\right|^2 \\ &= \frac{1}{2}(\partial_\mu H)^2 + \frac{1}{8}g_2^2(v+H)^2|W_\mu^1 + iW_\mu^2|^2 + \frac{1}{8}(v+H)^2|g_2W_\mu^3 - g_1B_\mu|^2 \end{aligned}$$

we can define and identify the new fields $W_\mu^\pm$ and Z_μ.

$$W^\pm = \tfrac{1}{\sqrt{2}}(W_\mu^1 \mp iW_\mu^2), \quad Z_\mu = \tfrac{g_2W_\mu^3 - g_1B_\mu}{\sqrt{g_2^2+g_1^2}}, \quad A_\mu = \tfrac{g_2W_\mu^3 + g_1B_\mu}{\sqrt{g_2^2+g_1^2}},$$

A_μ is the field orthogonal to Z_μ. If we pick up the terms which are bilinear in the fields $W^\pm$, Z, A, we get

$$M_W^2W_\mu^+W^{-\mu} + \frac{1}{2}M_Z^2Z_\mu Z^\mu + \frac{1}{2}M_A^2A_\mu A^\mu$$

where the W and Z bosons have acquired masses, while the photon is still massles

$$M_W = \tfrac{1}{2}vg_2, \quad M_Z = \tfrac{1}{2}v\sqrt{g_2^2+g_1^2}, \quad M_A = 0 \ .$$

Up to now, we have discussed only the generation of gauge boson masses, but in fact we can also generate the fermion masses using the same scalar field Φ, with hypercharge $Y = 1$, and the isodoublet $\tilde{\Phi} = i\tau_2\Phi^*$, which has hypercharge $Y = -1$. For any fermion generation, we introduce the $\mathrm{SU(2)_L \times U(1)_Y}$ invariant Yukawa Lagrangian

$$\mathcal{L}_F = -\lambda_e\overline{L}\Phi e_R - \lambda_d\overline{Q}\Phi d_R - \lambda_u\overline{Q}\tilde{\Phi}u_R + h.c.$$

Taking for instance the case of the electron, one obtains

$$\mathcal{L}_F = -\frac{1}{\sqrt{2}}\lambda_e(\overline{\nu}_e, \overline{e}_L)\begin{pmatrix} 0 \\ v + H \end{pmatrix}e_R + \cdots = -\frac{1}{\sqrt{2}}\lambda_e(v+H)\overline{e}_Le_R + \cdots$$

The constant term in front of $\overline{f}_Lf_R$ (and h.c.) is identified with the fermion mass

$$m_e = \tfrac{\lambda_e v}{\sqrt{2}}, \quad m_u = \tfrac{\lambda_u v}{\sqrt{2}}, \quad m_d = \tfrac{\lambda_d v}{\sqrt{2}}$$

What about Higgs? The kinetic part of the Higgs field, $\frac{1}{2}(\partial_\mu H)^2$, comes from the term involving the covariant derivative $|D_\mu \Phi|^2$, while the mass and self-interaction parts, come from the scalar potential $V(\Phi) = \mu^2 \Phi^\dagger \Phi + \lambda(\Phi^\dagger \Phi)^2$

$$V = \frac{\mu^2}{2}(0, v+H)\begin{pmatrix} 0 \\ v+H \end{pmatrix} + \frac{\lambda}{4}\left|(0, v+H)\begin{pmatrix} 0 \\ v+H \end{pmatrix}\right|^2$$

Using the relation $v^2 = -\mu^2/\lambda$, one obtains

$$V = -\frac{1}{2}\lambda v^2 (v+H)^2 + \frac{1}{4}\lambda (v+H)^4$$

and finds that the Lagrangian containing the Higgs field H is given by

$$\mathcal{L}_H = \frac{1}{2}(\partial_\mu H)(\partial^\mu H) - V = \frac{1}{2}(\partial^\mu H)^2 - \lambda v^2 H^2 - \lambda v H^3 - \frac{\lambda}{4} H^4.$$

From this Lagrangian, one can see that the Higgs boson mass simply reads

$$M_H^2 = 2\lambda v^2 = -2\mu^2$$

and the Feynman rules for the Higgs self interaction vertices are given by

$$g_{H^3} = (3!) i\lambda v = 3i\frac{M_H^2}{v}, g_{H^4} = (4!) i\frac{\lambda}{4} = 3i\frac{M_H^2}{v^2}$$

The Higgs boson couplings to gauge bosons and fermions are

$$g_{Hff} = i\frac{m_f}{v}, g_{HVV} = -2i\frac{M_V^2}{v}, g_{HHVV} = -2i\frac{M_V^2}{v^2}$$

The vacuum expectation value, v, is fixed in terms of the W boson mass M_W or the Fermi constant G_μ determined from muon decay.

$$M_W = \frac{1}{2} g_2 v = \left(\frac{\sqrt{2} g^2}{8 G_\mu}\right)^{1/2} \Rightarrow v = \frac{1}{(\sqrt{2} G_\mu)^{1/2}} \simeq 246\text{GeV}$$

4 Higgs production

4.1 Higgs production at lepton colliders

The e^+e^- collision is a very simple reaction, with a very well defined initial state and rather simple topologies in the final state. It has a favourable signal to background ratio, leading to a very clean experimental environment which

allows to easily search for new phenomena and to perform very high precision studies as has been shown at PEP/PETRA/TRISTAN and more recently at SLC and LEP.

The physical processes in e^+e^- collisions are in general mediated by s-channel photon and Z boson exchanges with cross sections which scale as the inverse of the center of mass energy squared, and t-channel gauge boson or electron/neutrino exchange, with cross-sections which may rise proportionally with the logarithm of the total center of mass energy. The s-channel exchange is the most interesting process when it takes place: it is democratic, in the sense that it gives approximately the same rates for weakly and strongly interacting matter particles, and for the production of known and new particles, when the energy is high enough. However, in this channel, the rates are low at high energies and one needs to increase the luminosity to compensate for the $1/s$ drop of the interesting cross sections. Also, another problem is that the synchroton radiation rises as the fourth power of the c.m. energy in circular machines so the e^+e^- colliders beyond LEP2 must be linear machines.

In e^+e^- collisions with center of mass energies beyond LEP2, the main production mechanism for Higgs particles are the so-called Higgs-strahlung process and the WW fusion mechanism. There are several other mechanisms in which Higgs bosons can be produced in e^+e^- collisions: the ZZ fusion process, the radiation of top quarks, and the double Higgs boson production process either in Higgs-strahlung or WW/ZZ fusion. But these are, in principle, higher order processes in the electr-weak coupling with production cross-sections much smaller than those of the Higgs-strahlung and WW fusion fusion channel. However, with the high luminosity planned for future linear colliders, they can be detected and studied.

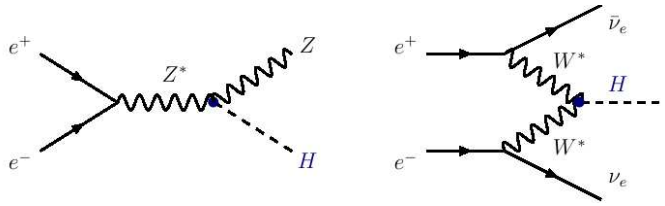

Figure 1: The dominant Higgs production mechanisms in high-energy e^+e^- collisions.

The production cross-section for the Higgs-strahlung process is given by

$$\sigma(e^+e^- \to ZH) = \frac{G_\mu^2 M_Z^4}{96\pi s}(\hat{v}_e^2 + \hat{a}_e^2)\lambda^{1/2}\frac{\lambda + 12M_Z^2/s}{(1 - M_Z^2/s)^2}$$

where, $\hat{a}_e = -1$ and $\hat{v}_e = -1 + 4s_W^2$ are the Z charges of the electron and $\lambda^{1/2}$ the usual two-particle phase-space function

$$\lambda = (1 - M_H^2/s - M_Z^2/s)^2 - 4M_H^2 M_Z^2/s^2$$

The production cross-section is shown in the figure 2 as a function of the Higgs

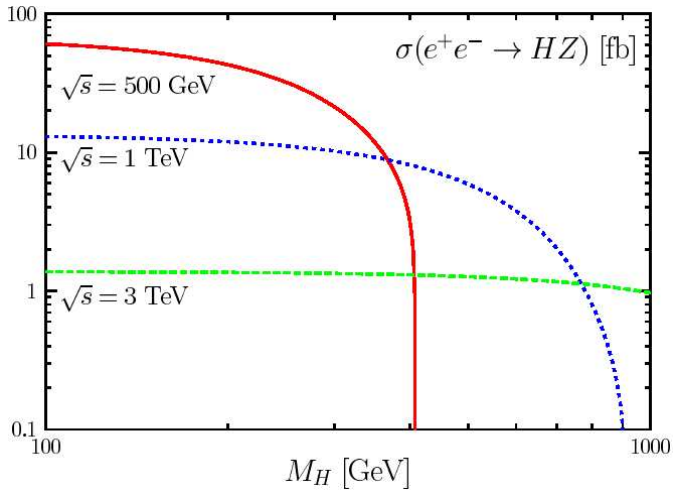

Figure 2: Higgs boson production cross-sections in the Higgs-strahlung mechanism in e^+e^- collisions with c.m. energies $\sqrt{s}$= 0.5, 1 and 3 TeV as a function of M_H.

mass for the values of the c.m. energy $\sqrt{s}$ =0.5, 1 and 3 TeV. The maximum value of the cross-section for a given M_H value is at $\sqrt{s} \sim M_Z + \sqrt{2}M_H$. An energy of the order of 800 GeV is needed in order to cover the entire Higgs boson mass range allowed in the SM, $M_H <\sim 700$GeV.

The recoiling Z boson in the two-body reaction $e^+e^- \to ZH$ is mono-energetic, and the mass of the Higgs boson can be derived from the energy of the Z boson, $M_H^2 = s - 2\sqrt{s}E_Z + M_Z^2$, if the initial e^+ and e^- beam energies are sharp.

The angular distribution of the Z/H bosons in the bremsstrahlung process is also sensitive to the spin of the Higgs particle. The explicit form of the angular distribution, with θ being the scattering angle, is given by

$$\frac{d\sigma(e^+e^- \to ZH)}{d\cos\theta} \sim \lambda^2 \sin^2\theta + 8M_Z^2/s \overset{s \gg M_Z^2}{\to} \frac{3}{4}\sin^2\theta$$

and approaches the spin-zero distribution asymptotically.

The WW fusion process is most important for small values of the ratio $M_H/\sqrt{s}$, ii.e. high energies, where the cross section grows $\sim M_W^{-2}\log(s/M_H^2)$. The production cross-section, can be conveniently written as

$$\sigma = \frac{G_\mu^3 M_V^4}{64\sqrt{2}\pi^3}\int_{k_H}^1 dx \int_x^1 \frac{dy}{[1+(y-x)/\kappa_V]^2}[(\hat{v}_e^2+\hat{a}_e^2)^2 f(x,y) + 4\hat{v}_e^2\hat{a}_e^2 g(x,y)]$$

$$f(x,y) = \left(\frac{2x}{y^3} - \frac{1+2x}{y^2} + \frac{2+x}{2y} - \frac{1}{2}\right)\left[\frac{z}{1+z} - \log(1+z)\right] + \frac{x}{y^3}\frac{z^2(1-y)}{1+z}$$

$$g(x,y) = \left(-\frac{x}{y^2} + \frac{2+x}{2y} - \frac{1}{2}\right)\left[\frac{z}{1+z} - \log(1+z)\right]$$

where $\kappa_H = m_H^2/s$, $\kappa_V = M_V^2/s$, $z = y(x-\kappa_H)/(\kappa_V x)$ and $\hat{v}$, $\hat{a}$ the electron couplings to the massive gauge bosons, $\hat{v}_e = \hat{a}_e = \sqrt{2}$ for the W boson.

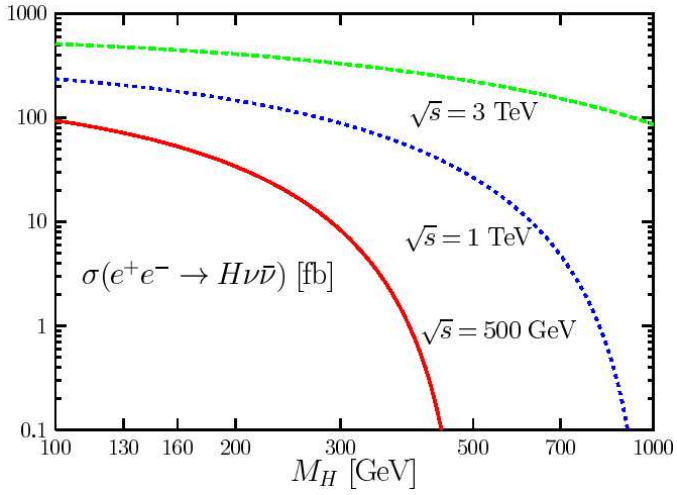

Figure 3: The Higgs production cross section in the WW fusion mechanisms e^+e^- collisions with c.m. energies $\sqrt{s}$ =0.5, 1 and 3 TeV as a function of M_H.

The production cross section is shown in the figure 3 as a function of M_H at c.m. energies $\sqrt{s}$ =0.5, 1 and 3 TeV. For Higgs masses in the intermediate range, the cross section is comparable to the one of the Higgs-strahlung process at $\sqrt{s} = 500$ GeV.

4.2 Higgs production at hadron colliders

The $p\overline{p}$ collider Tevatron at Fermilab is the highest energy accelerator available today. This collider operated in Run I at a nominal energy of $\sqrt{s}$ =1.8

TeV and was upgraded for Run II at $\sqrt{s}$ =1.96 TeV which, typically, increased the cross sections for some physics processes by about 30%.

The CERN Large Hadron Collider (LHC) under construction is a pp collider designed to run at an energy $\sqrt{s}$ =14TeV in the pp center of mass. The first collisions are expected in June 2007, but in a lower than nominal luminosity regime. There are also plans for an upgrade of the LHC magnets which can double this c.m. energy. Currently there are studies for a very large hadron collider (VLHC) which can move the $\sqrt{s}$ limits up to 40-200 TeV.

The two general purpose experiments under construction, ATLAS and CMS, have been optimized to cover a large spectrum of possible signatures in the LHC environment.

Unlike lepton colliders, the total cross-section at hadron colliders is extremely large. It is about 100mb at LHC, resulting in an interaction rate of $\approx 10^9$Hz at the design luminosity. In this hostile environment, the detection of processes with signal to total hadronic cross section ratios of about 10^{-10}, as is the case for the production of SM Higgs boson in most channels, will be a difficult experimental challenge.

In the Standard Model, the main production mechanisms for Higgs particles at hadron colliders make use of the fact that Higgs boson couples preferentially to the heavy particles, that is the massive W and Z vector bosons, the top quark and, to a lesser extent, the bottom quark. The four main production processes, the Feynman diagrams of which are displayed in figure 4 , are thus: the associated production with W/Z bosons, the weak

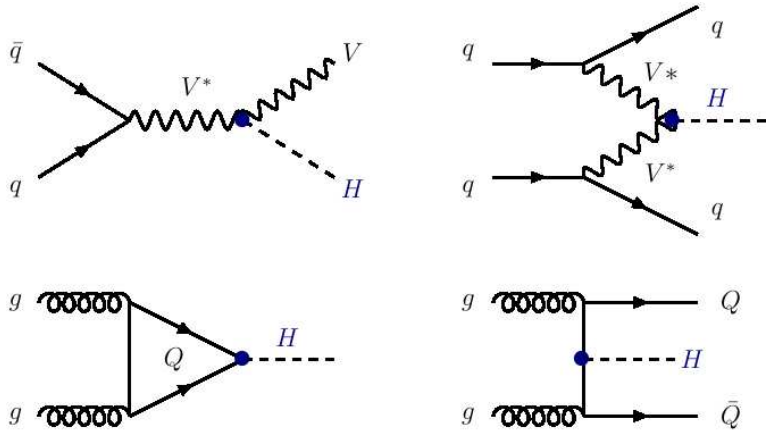

Figure 4: The dominant Higgs boson production mechanisms in hadronic collisions.

vector boson fusion processes, the gluon-gluon fusion mechanism and the associated Higgs production with heavy top or bottom quarks. There are also several mechanisms for the pair production of the Higgs particles involving associated vector bosons or quark pairs production. However, this type of processes are suppresed due to the additional weak couplings. Also suppresed are processes where the Higgs is produced in association with one, two or three hard jets in gluon-gluon fusion, etc. Finally, Higgs boson can also be produced in diffractive processes. This mechanism is mediated by color singlet exchanges leading to the diffraction of the incoming hadrons and a centrally produced Higgs boson.

4.2.1 The associated production with W/Z bosons

This process can be viewed simply as the Drell-Yan production of a virtual vector boson with $k^2 \neq M_V^2$, which then splits into a real vector boson and a Higgs particle.

$$q_1(p_1) + \overline{q}_2(p_2) \rightarrow V^*(k = p_1 + p_2) \rightarrow V(k_1) + H(k_2)$$

In the case where the decay products of the final vector boson are ignored, one would have a simple $2 \rightarrow 2$ subprocess, with an integrated cross section at lowest order given by

$$\hat{\sigma}_{LO}(q\overline{q} \rightarrow VH) = \frac{G_\mu^2 M_V^4}{288\pi\hat{s}}(\hat{v}_q^2 + \hat{a}_q^2)\lambda^{1/2}(M_V^2, M_H^2; \hat{s})\frac{\lambda(M_V^2, M_H^2; \hat{s}) + 12M_V^2/\hat{s}}{(1 - M_V^2/\hat{s})^2}$$

where the reduced fermion couplings to gauge bosons are: $\hat{a}_f = 2I_f^3$, $\hat{v}_f = 2I_f^3 - 4Q_f s_W^2$ for $V = Z$ and $\hat{v}_f = \hat{a}_f = \sqrt{2}$ for $V = W$. The total production cross section is then obtained by convoluting with the parton densities and summing over the contributing partons. Using a set of parton distribution functions (PDFs), one can make a Monte-Carlo simulation in order to obtain the total cross section. In figure 5 the total cross-sectio for the discussed process as a function of Higgs mass is ilustrated.

4.2.2 The vector boson fusion process

The cross sections for this process, using CTEQ set of parton densities, are shown in figure 6 as a function of M_H for $p\overline{p}$ at the Tevatron and for pp at the LHC. In the later case, the separate WW and ZZ contributions, as well as their total sum, are displayed. While they are rather large at the LHC, in particular for Higgs bosons in the mass range 100 GeV ¡ M_H ¡ 200 GeV where they reach the level of a few picobarns, the total cross sections are

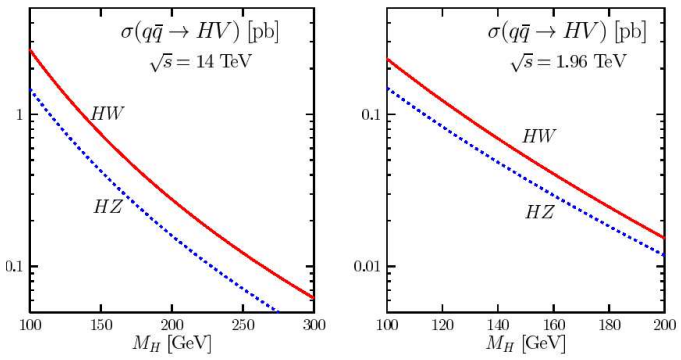

Figure 5: The total production cross sections of Higgs bosons in the strahlung processes at leading order at the LHC(left) and at the Tevatron (right). For $H \to HW$, the final states with both W^+ and W^- have been added. The MRST set of PDFs have been used.

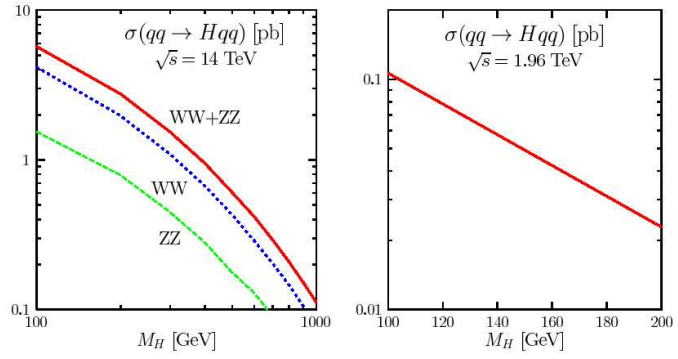

Figure 6: Individual and total cross sections in the vector fusion $qq \to V^*V^* \to Hqq$ process at leading order at the LHC(left) and total cross section at the Tevatron(right).

very small at the Tevatron and they barely reach the level of 0.1 pb even for $M_H = 100$ GeV. Note also that the main contribution to the cross section is due to the WW fusion channel, $\sigma(WW \to H) \sim 3\sigma(ZZ \to H)$ at the LHC, a consequence of the fact that the W boson couplings to fermions are larger that those of the Z boson.

4.2.3 The gluon-gluon fusion mechanism

Higgs production in the gluon-gluon fusion mechanism is mediated by triangular loops of heavy quarks. In the SM, only the top quark and, to a lesser extent, the bottom quark will contribute to the amplitude. The decreasing Hgg form factor with rising loop mass is counterbalanced by the linear growth of the Higgs coupling with the quark mass.

The total hadronic cross sections at LO are shown in figure 7 as a function

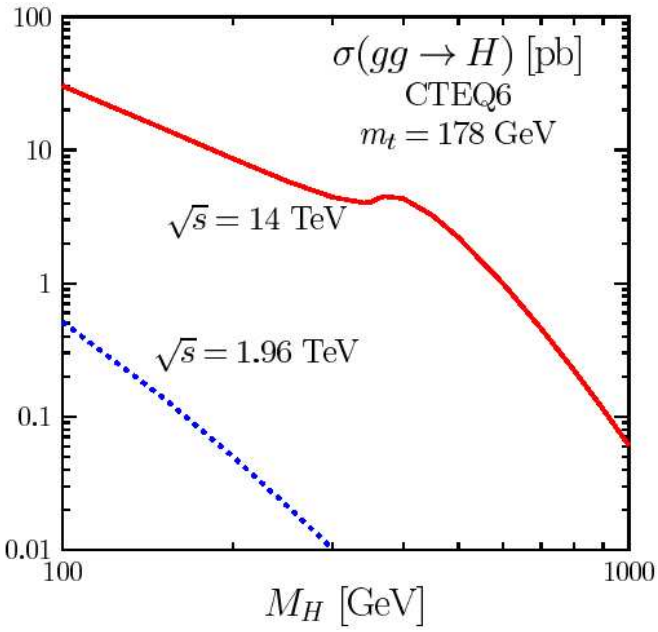

Figure 7: The hadronic production cross sections for the gg fusion process at LO as a function of M_H at the LHC and at the Tevatron. The inputs are m_t=178GeV, m_b =4.88GeV, the CTEQ set of PDFs has been used and the scalesare fixed to $\mu_R = \mu_F = M_H$.

of the Higgs boson mass. We have chosen m_t =178GeV, m_b =4.88GeV and $\alpha_s(M_Z)$ =0.13 as inputs and used the CTEQ parametrization for the parton densities. For the Tevatron, the rates monotonically decreasing with the

Higgs mass, starting slightly below 1pb for M_H ∼100GeV. At the LHC, the cross section is two order of magnitude larger, but is also decreasing with Higgs mass and additionally there is a kink around M_H ∼350GeV, near the $t\bar{t}$ threshold where the Hgg amplitude develops an imaginary part.

4.2.4 Associated Higgs production with heavy quarks

The process where the Higgs boson is produced in association with heavy quark pairs, $pp \to Q\overline{Q}H$, with the final state quarks being either the top quark ot the bottom quark, is the most involved of all SM Higgs production mechanisms. At tree level, it originates from $q\overline{q}$ annihilation into heavy quarks with the Higgs boson emitted from the quark lines; this is the main source at Tevatron energies. At higher energies, when the gluon luminosity becomes important, the process proceeds mainly trough gluon fusion, with the Higgs boson emitted from both the external and internal quark lines (see figure 8). The cross section for associated $t\bar{t}H$ and $b\bar{b}H$ production are shown

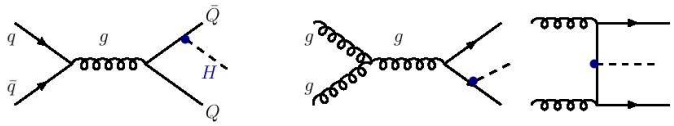

Figure 8: Generic Feynman diagrams for associated Higgs production with heavy quarks in hadronic collisions, $pp \to q\overline{q}, gg \to Q\overline{Q}H, at LO$.

in 9 for the Tevatron and LHC energies. The MRST set of parton densities

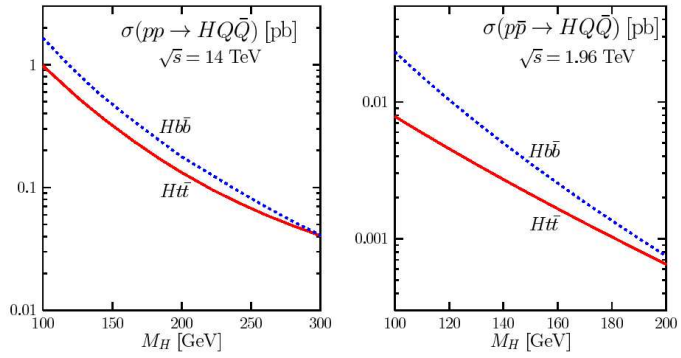

Figure 9: The $t\bar{t}H$ and $b\bar{b}H$ production cross sections at the LHC(left) and at the Tevatron (right).

has been used and the renormalization and factorization scales have been

identified with μ_R=μ_F=$m_Q + \frac{1}{2}m_H$ and $\frac{1}{4}M_H$ for the $t\bar{t}H$ and $b\bar{b}H$ cases, respectively. As can be seen, the $p\overline{p} \to t\bar{t}H$ cross section at the Tevatron is of the order of 5 fb for small Higgs masses and decreases with increasing mass of Higgs. At the LHC, the cross section is two orders of magnitude larger as a consequence of the higher energy, higher gluon luminosity and larger phase space.

5 Higgs decays

In the previous section we discussed the most important Higgs boson production processes. Now we will study the way, the Higgs boson decays. We first consider Higgs decay into fermions.

5.1 Higgs decay into fermion-anti-fermion

The decay amplitude for this channel is

$$T_{fi} = \frac{g}{2M_W} m_f \overline{v}^{s2}(k_2) u^{s_1}(k_1).$$

The matrix element squared is

$$|\mathcal{M}|^2 = \sum_{s_1,s_2} |T_{fi}|^2,$$

where $|T_{fi}|^2 = T_{fi}T_{fi}^{\dagger}$. The squared amplitude becomes

$$|\mathcal{M}|^2 = \frac{g^2}{4M_W^2} m_f^2 \sum_{s_1,s_2} \overline{v}^{s_2}(k_2) u^{s_1}(k_1) \overline{u}^{s_1}(k_1) v^{s_2}(k_2)$$

$$= \frac{g^2}{4M_W^2} m_f^2 \sum_{s_2} \overline{v}^{s_2}(k_2) \sum_{s_1} u^{s_1}(k_1) \overline{u}^{s_1}(k_1) v^{s_2}(k_2)$$

$$|\mathcal{M}|^2 = \frac{g^2}{4M_W^2} m_f^2 \mathrm{Tr}\{(k_{1\mu}\gamma^{\mu} + m_f)(k_{2\nu}\gamma^{\nu} - m_f)\} = \frac{g^2}{4M_W^2} m_f^2 [4k_1k_2 - 4m_f^2]$$

The decay kinematic is simple in the rest mass of the Higgs boson.

$$k_1 = (m_H/2, \vec{k}_1) \quad k_2 = (m_H/2, \vec{k}_2)$$

$$k_1k_2 = m_H^2/4 - \vec{k}_1\vec{k}_2 = m_H^2/4 + |\vec{k}_1||\vec{k}_2| = m_H^2/4 + |\vec{k}|^2 = m_H^2/2 - m_f^2$$

So, the squared amplitude has the form

$$|\mathcal{M}|^2 = \frac{g^2}{2M_W^2} m_f^2 [m_H^2 - 4m_f^2]$$

The two-body decay width is

$$\begin{aligned} d\Gamma &= |\mathcal{M}|^2 \frac{|\vec{p}_1|}{E_H^2} \frac{d\Omega_1}{32\pi^2} \\ &= \frac{\sqrt{m_H^2/4 - m_f^2}}{m_H^2} \frac{d\Omega_1}{32\pi^2} \frac{g^2}{2m_W^2} m_W^2 (m_H^2 - 4m_f^2) \\ &= \frac{g^2}{4m_W^2} m_f^2 m_H \left(1 - \frac{4m_f^2}{m_H^2}\right)^{\frac{3}{2}} \frac{d\Omega_1}{32\pi^2} \end{aligned}$$

Finally, we can integrate over $d\Omega$ and obtain the width

$$\Gamma = \frac{g^2}{32\pi} \frac{m_f^2}{m_W^2} m_H \left(1 - \frac{4m_f^2}{m_H^2}\right)^{3/2} \times N_c^f$$

where we added a colour factor which is 3 for quarks and 1 for leptons.

5.2 Higgs decay into weak gauge boson pairs

The Higgs boson couplings to the weak gauge bosons are $g_{HWW} = g m_W$ and $g_{HZZ} = g \frac{m_Z}{\cos\theta_W}$. The matrix element for this type of process is

$$T_{fi} = g_{HVV} \epsilon_\mu^*(k_1, \lambda_1) \epsilon^\mu(k_2, \lambda_2)$$

The calculation of the squared amplitude and decay widths for both processes are straightforward. We will just show the final results:

$$\begin{aligned} \Gamma(H \to W^+W^-) &= \frac{G_F}{8\pi\sqrt{2}} m_H^3 \left(1 - \frac{4m_W^2}{m_H^2}\right)^{\frac{1}{2}} \left[3\left(\frac{m_W^2}{m_H^2}\right)^2 - 4\left(\frac{m_W^2}{m_H^2}\right) + 1\right] \\ \Gamma(H \to Z^0Z^0) &= \frac{G_F}{16\pi\sqrt{2}} m_H^3 \left(1 - \frac{4m_Z^2}{m_H^2}\right)^{\frac{1}{2}} \left[3\left(\frac{m_Z^2}{m_H^2}\right)^2 - 4\left(\frac{m_Z^2}{m_H^2}\right) + 1\right] \end{aligned}$$

Up to some extent, its easy to see from the above formulas and from the figure that the decay width of the Higgs into W bosons is twice the decay width into Z bosons.

Some indirect experimental limits for Higgs mass were obtained from precision measurements of the electroweak parameters which depend logarithmically on the Higgs boson mass through radiative corrections. Figure 10 shows the $\Delta\chi^2$ curve derived from the precision electroweak measurements, performed at LEP and by SLD, CDF, D0, NuTeV and others as a function of the Higgs boson mass. The preferred value for its mass, corresponding to the minimum of the curve, is

$$\begin{aligned} m_H &= 81^{+52}_{-33}\text{GeV} \\ m_H &= 96^{+60}_{-38}\text{GeV} \end{aligned}$$

at 68% CL derived from $\Delta\chi^2 = 1$ for the black line, thus not taking into account the theoretical uncertainty shown as the blue band.

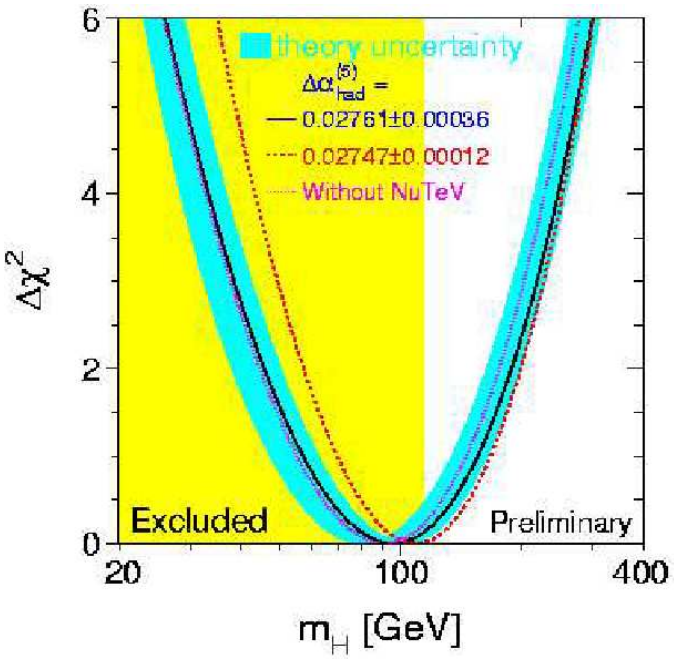

Figure 10: $\Delta\chi^2$ curve as a function of m_H.

6 How to hunt a Higgs?

6.1 General considerations on the Higgs search strategy

In the previous sections we discussed the theoretical aspects regarding the Higgs boson. We know, at least approximately, how and how many Higgs will be produced through the different processes. We also know, again, at least approximately, how a produced Higgs decays in more or less stable particles which can be detected by the experiment.
So, it seems that the things looks good :). Unfortunately, from the experimental point of view, to track down the Higgs boson is a very delicate job. The total pp cross section at LHC energies is about 100mb while the most prolific Higgs production mechanism is lying around a cross section of about 50pb. To be able of such a performance, one needs very precise detectors. Also, because of the very dirty nature of hadronic interactions, the sources of background must be known very well in order to be substracted from the final cross-sections. The last, but not the least important ingredient of the Higgs search strategy, is STATISTICS!!
In order to obtain a good signal to background ratio, we must acumulate

a huge amount of events. After carefull estimations, the CMS and ATLAS detectors are designed to discover the SM Higgs for all masses ¡ 1TeV in four months of full luminosity operation. This is assumed to occur if a significance of about five standard deviations is achieved.

Depending on the rarity of the final state with respect to the specific backgrounds existing for that particular final state, different production mechanisms may be needed on a case-by-case basis if we are to fashion a successful search strategy. That strategy is very dependent on the unknown Higgs mass. For example, a basic issue is wheter the Higgs mass is sufficient to use the relatively straightforward ZZ final state or not. The figure 11 shows the

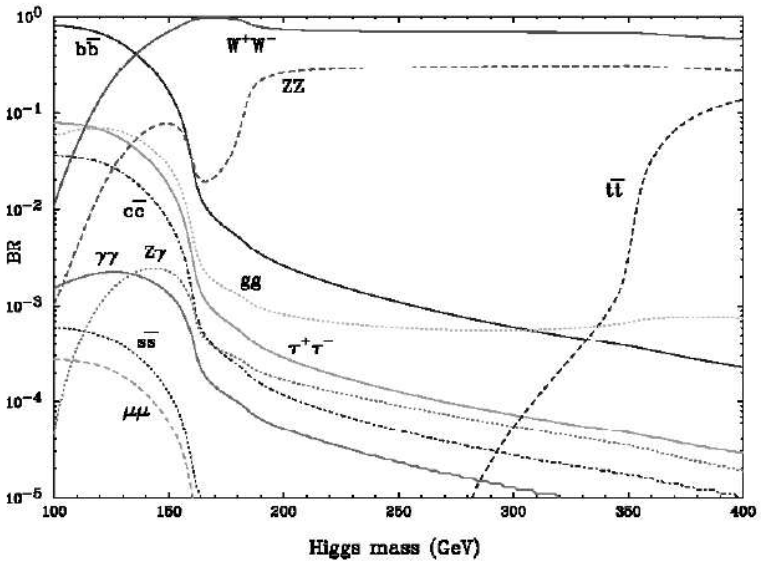

Figure 11: Branching ratios of the Higgs boson as a function of the Higgs boson mass.

branching ratios for the Higgs boson as a function of the Higgs mass. It's easy to observe how fast, the branching ratios are varying with the Higgs mass.

The Higgs width is very small below the WW threshold. The widths into quarks scale as the square of the quark mass. Hence the heaviest available quark pair, $b\overline{b}$, dominates below WW threshold at a mass of ~ 130 GeV. The charm pair branching ratio is estimated to be $B(c\overline{c}) \sim (m_c/m_b)^2 B(b\overline{b}) \sim 0.1$. The heaviest accesible lepton pair, τ, has a width reduced by $\sim$9 relative to the b pair width because of the coupling to mass squared , and by a 1/3 color factor, leading to a rough estimate of the branching fraction of 1/27. The

$\gamma\gamma$ channel has a branching ratio estimate of 0.00019 while the gg branching ratio is about 0.04 at low Higgs masses.

Decay widths generated with COMPHEP are shown in figure 12 The top pair width, because the mass is so large, can be substantial, but this branching ratio has a very high threshold.

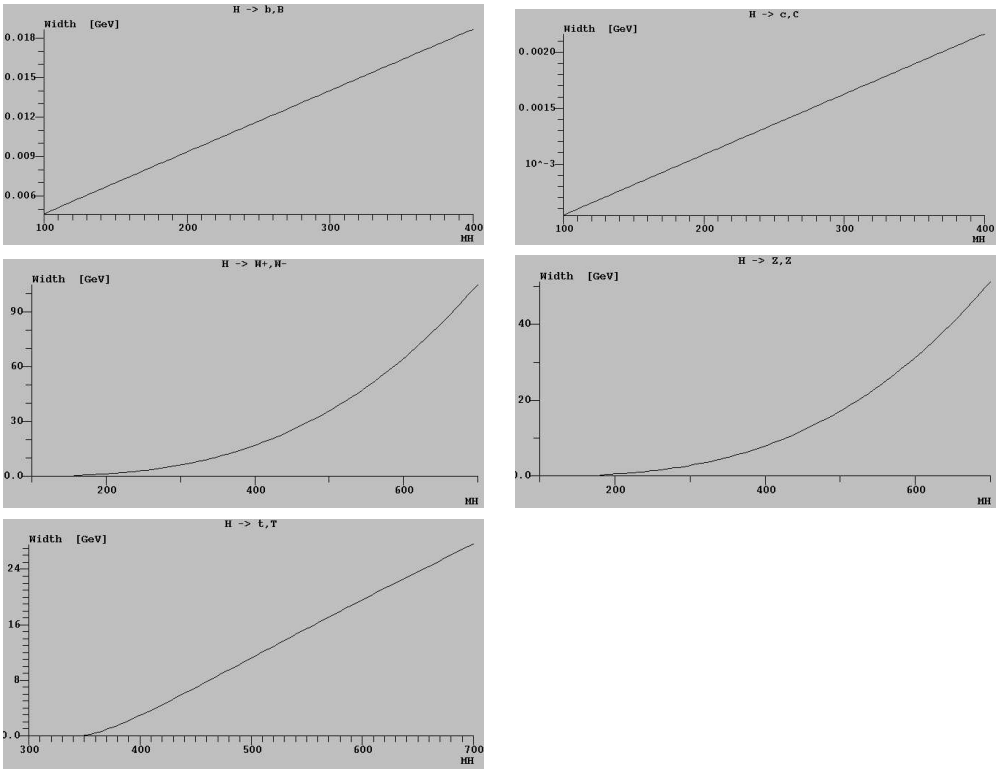

Figure 12: Higgs boson decay width through different channels as a function of Higgs mass. The distribution were generated using COMPHEP. Upper row:$H \to b\overline{b}$ (left), $H \to c\overline{c}$ (right); middle row: $H \to W^+W^-$(left), $H \to Z^0Z^0$(right); bottom row: $H \to t\overline{t}$.

Around a Higgs mass of ∼150GeV, we start to have an important contribution from the below ZZ threshold decays into the Zl^+l^- with an off-shell Z, conventionally called ZZ^*. The decay width of this channel at 160GeV is about 0.5 MeV, while the width for the WW^* channel is 6 MeV which is approximately the b pair width.

The widths above WW and ZZ threshold generated with COMPHEP, are shown in figure 12 These widths have a $\Gamma \sim M^3$ behaviour and at a mass of

Higgs boson around 600 GeV, the decay widths into heavy particles are big.

$$\Gamma(H \to WW) = 70GeV$$
$$\Gamma(H \to ZZ) = 35GeV$$
$$\Gamma(H \to t\bar{t}) = 20GeV$$

Of the decay modes mentioned so far, the $H \to \gamma\gamma$ decay mode is a clean method to search for low mass Higgs. The b pair and τ pair decay modes are also accesible at low mass if the ttH (associated production) and qqH (WW fusion with tag jets) production mechanisms are employed respectively. Above an effective threshold for ZZ^* at ∼150GeV Higgs mass the four lepton mode is clean and is the process of choice. The WW decay to two leptons and two neutrinos does not have a sharp transverse mass peak due to loss of information about the longitudinal momentum of the neutrinos. Nevertheless with the use of tag jets to signal WW fusion production, the $H \to W + W^* \to (l^+ + \nu_l) + (l^- + \overline{\nu}_l)$ decay is a major discovery mode for Higgs particles with mass <200 GeV.

6.2 Using $b\overline{b}$ decay channel to discover Higgs

As we concluded in the earlier section, the $b\overline{b}$ final state for a Higgs boson is the most probable at low Higgs masses. But is not the cleanest!! There is a strong QCD background coming from the much more probable processes that can happen in a pp collision without involving the production of a Higgs boson. But, by knowing the Higgs production mechanisms, we can impose special conditions on the events, in order to cut most of the background.

We assume that the b dijet invariant mass is calorimetrically reconstructed for a Higgs mass of 120GeV, where the cross section is 30 pb, with a 3 standard deviation ($\pm 1.5\sigma$) signal region of $b\overline{b}$ mass, ΔM = 22 GeV set by the experimental resolution of the calorimetry. Thus, the signal appears as a, $\sigma/\Delta M = 30$ pb/22 GeV = 1.4 pb/GeV, resonant bump above the continuum cross section for the QCD production of b quark pairs (we assume that the 120 GeV Higgs b pair branching fraction is 1).

The COMPHEP Feynman diagrams for the QCD production of continuum b quark pairs are shown in figure 13

The predicted cross section at the LHC is shown in figure 14 The signal is also indicated there. It is swaped by a factor of ∼1000. It is for this reason that we were forced to consider Htt production with subsequent $H \to b + \overline{b}$ decay, where the signal to background ratio is much more favorable. Using the associated production mechanism, we can extract the cross section times $b\overline{b}$ branching ratio for light Higgs bosons and thus measure the Higgs coupling to b quarks.

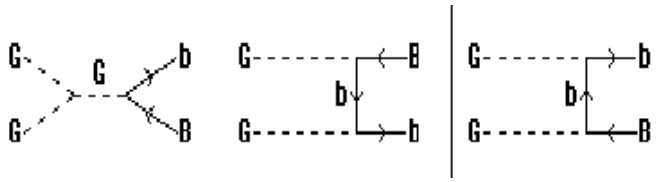

Figure 13: COMPHEP Feynman diagrams for the process $g + g \rightarrow b + \overline{b}$.

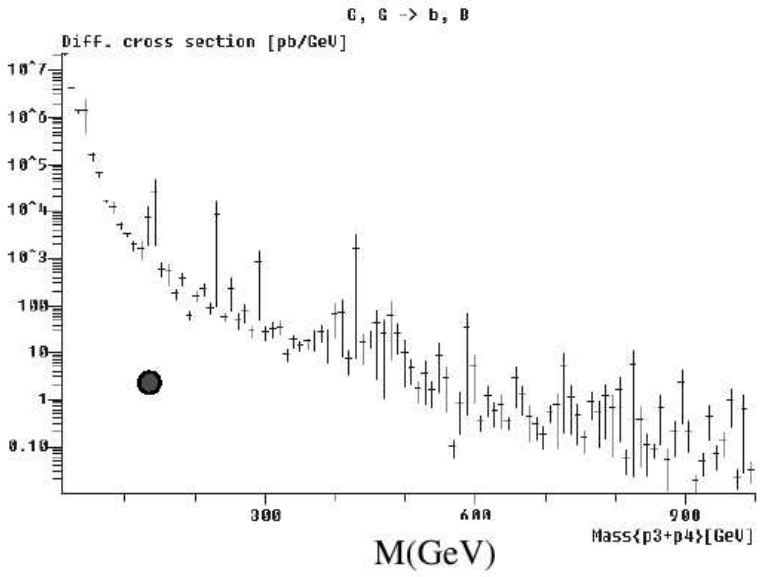

Figure 14: COMPHEP prediction for the production of b quark pairs at LHC as a function of the quark pair mass. The dot represents the Higgs signal level for a 120 GeV mass Higgs.

7 Why go beyond the Standard Model?

Actually, there are many reasons why the electroweak theory cannot have the final word. For one, the standard model is largely silent on the issue of the origin of the Higgs boson, and this is because the spontaneous breaking of the electroweak SU(2)xU(1) symmetry is postulated in the model by the device of introducing a potential of scalar fields, $V(\phi)$, constructed just so that it can lead to such a breaking. And the condition for this to happen is $\mu^2 < 0$. This raises the question, what drives μ^2 negative? Clearly the answer, if any, lies beyond the realm of the model, perhaps in some more complex, even fundamental mechanism.

We can summarize some important points that can be drawn from the actual Standard Model:

* The Higgs boson is necessary to regulate the E^2-growth of the amplitudes, otherwise unitarity would be violated.

* If a Higgs boson can be found in future experiments with a relatively small mass, say $M_H < v = 246$ GeV, then we are in the weakly coupled regime of λ and the theory remains consistent. But the question why $\mu^2 < 0$ will remain unanswered.

* However, if the Higgs boson is too heavy, i.e., if the coupling constant $\lambda \gg 1$, terms of higher orders in λ become increasingly more important and will get out of control, and the perturbative approach loses its usefulness.

All of these considerations strongly hint at the posibility that the electroweak standard model would somehow be embedded in a more fundamental theory. Which one, that is the most compelling question of today's particle physics.

8 References

For this project i used the following works:

- Elementary Particles and their interactions: Concepts and phenomena; Quang Ho-Kim, Xuan-Yem Pham; Springer 2004

- High Pt physics at hadron colliders; Dan Green; Cambridge University Press 2004

- Elementary particle physics - lecture notes; Farid Ould-Saada; University of Oslo
- The Anatomy of electro-weak symmetry breaking; Abdelhak Djouadi; hep-ph/0503172v2; 2005
- The Standard Model of electroweak interactions; A.Pich; hep-ph/0502010v1; 2005
- The Standard Model: Physical basis and scattering experiments; H.Spiesberger, M.Spira, P.M.Zervas; hep-ph/0011255v1; 2000